Highlights on Spanish Astrophysics X, Proceedings of the XIII Scientific Meeting of the Spanish Astronomical Society held on July 16 – 20, 2018, in Salamanca, Spain. B. Montesinos, A. Asensio Ramos, F. Buitrago, R. Schödel, E. Villaver, S. Pérez-Hoyos, I. Ordóñez-Etxeberria (eds.), 2019

Inference of physical parameters in solar prominence threads.

M. Montes-Solís[1,2], **I. Arregui**[1,2]

[1] Instituto de Astrofísica de Canarias, E-38205 La Laguna, Tenerife, Spain
[2] Departamento de Astrofísica, Universidad de La Laguna, E-38206 La Laguna, Tenerife, Spain

Abstract

We consider magnetohydrodynamics models and observations of transverse oscillations in prominence threads to obtain information on their physical properties such as the magnetic field strength, the plasma density, or the length. We further compare between short and long thread limits in period ratio models and compute the relative plausibility of alternative mechanisms in explaining the observed damping of transverse oscillations. Bayesian techniques are used for both analyses. The results show that the physical parameters of interest can be inferred. Values of period ratio around 1 are more likely in the long thread limit while shorter and larger values are more likely in the short thread limit. The mechanism known as resonant absorption in the Alfvén continuum is the most plausible damping mechanism.

1 Introduction

High-resolution observations have permitted to resolve fine-structure of prominences as threads that support transverse oscillations and flows [4, 5, 6]. In the last years, coronal seismology has been used to infer properties of the solar corona and structures therein, such as prominence threads [2]. In this work, we apply Bayesian techniques to the study of transverse kink oscillations in prominence threads to infer some of their physical features. In particular, if we take a model M with n parameters θ and some data d, these techniques enable us to infer the posterior distribution of each parameter or marginal posterior as

$$p(\theta_i|M,d) = \int p(\theta|M,d)d\theta_1...d\theta_{i-1}d\theta_{i+1}...d\theta_n, \tag{1}$$

where $p(\theta|M,d)$ is given by the Bayes' Rule in the form

$$p(\theta|M,d) = \frac{p(\theta)p(d|M,\theta)}{p(d|M)}. \tag{2}$$

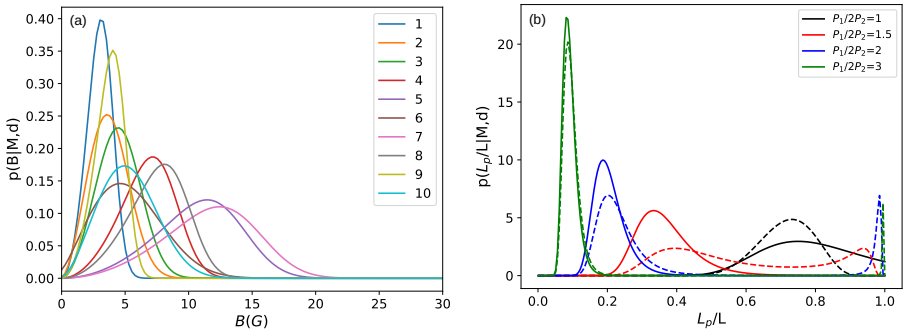

Figure 1: (a) Posterior distributions of magnetic field strength corresponding to the threads observed by [4]. Parameters are considered in plausible ranges of $B \in [0.01, 50]$ G and $\rho_p \in [10^{-12}, 10^{-9}]$ kg m^{-3}. (b) Posterior distributions of L_p/L for different $P_1/2P_2$ values with an uncertainty of 10% in the long thread limit. $L_p/L \in (0, 1)$ has been selected as plausible range. The continuous lines correspond to results using the first equation in (5) and dashed lines to the second one.

Including then the prior information, $p(\theta)$, the likelihood of the data, $p(d|M, \theta)$, and the normalization constant or marginal likelihood, $p(d|M)$, we can extract the probability of each parameter taking on certain values. On the other hand, Bayesian statistics allows us to compare plausibilities between alternatives mechanisms M_i and M_j with the computation of the Bayes' factors defined by

$$B_{ij} = \frac{p(d|M_i)}{p(d|M_j)}. \tag{3}$$

This relation of marginal likelihoods indicates which model better explains the observations.

2 Parameter inference

2.1 Magnetic field strength

Our first analysis is focused on the inference of the magnetic field strength in prominence threads. Assuming threads as totally filled thin tubes, theory predicts a phase velocity of transverse waves, v_{ph}, as a function of the magnetic field strength, B, and the density of the thread, ρ_p, in the form

$$v_{ph} = \sqrt{\frac{2}{\mu_0 \rho_p}} B, \tag{4}$$

if the density contrast between the thread and the background corona is sufficiently large.

Applying Bayesian techniques, marginal posteriors of the two unknowns $\theta = \{B, \rho_p\}$ can be computed, conditional on the observed phase velocity, $d = v_{ph}$ and the theoretical model. Figure 1a shows posterior distributions of the magnetic field strength associated to different threads whose phase velocities were measured by [4].

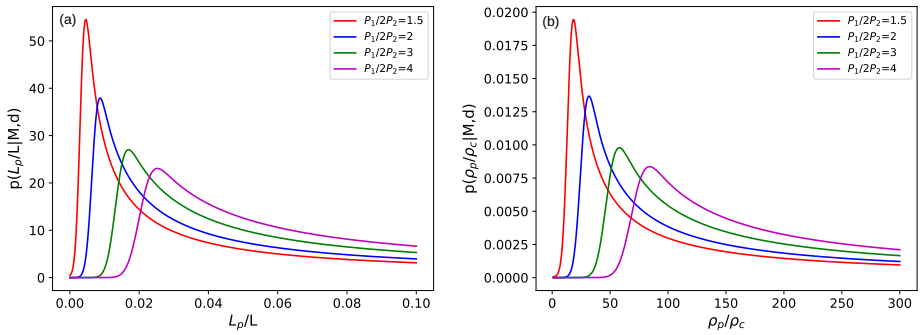

Figure 2: Posterior distributions of (a) L_p/L and (b) ρ_p/ρ_c for different $P_1/2P_2$ values with an uncertainty of 10% in the short thread limit.$L_p/L \in [0, 0.1]$ and $\rho_p/\rho_c \in [1.01, 300]$ has been selected as plausible ranges of parameters.

All 10 distributions can be properly inferred. They spread over a range of values although threads are in the same quiescent prominence and a very small probability of magnetic field strengths larger than 20 G is appreciable.

2.2 Lengths and densities in a partially filled tube

Our second analysis considers the relation between the periods of the fundamental and first overtone of transverse waves, $d = P_1/2P_2$, as a seismological tool. Assuming threads as partially filled thin tubes, theory [3] offers analytical expressions of the period ratio as a function of the thread length under two different approximations. In the long thread approximation, it can be approximated as

$$\frac{P_1}{2P_2} \approx \sqrt{\frac{3}{4L_p/L}} \text{ or } \frac{P_1}{2P_2} \approx \sqrt{\frac{3}{4L_p/L}} \sqrt{\frac{1+\sqrt{(1+L_p/3L)/(1-L_p/L)}}{1+\sqrt{(9/5-L_p/L)/(1-L_p/L)}}}, \tag{5}$$

both depending on only one parameter, the ratio of the length of the thread to the length of the tube, $\theta = \{L_p/L\}$. Marginal posteriors computed for different values of the period ratio are plotted in Figure 1b. The distributions are centred around smaller values of the parameter for longer values of the period ratio. The largest discrepancies between both equations in (5), are obtained for the longest threads. If we now focus on the short thread limit, the theoretical periods ratio can be expressed in the following manner

$$\frac{P_1}{2P_2} \approx 1 + (f^2-2)\frac{L}{L_p} - (f^2+1)\left(\frac{L}{L_p}\right)^2. \tag{6}$$

The equation depends on two parameters, the previous one and the density contrast between the thread and the corona through $f = \sqrt{(\rho_p/\rho_c+1)/2}$, hence $\theta = \{L_p/L, \rho_p/\rho_c\}$. Repeating the process, we obtain their marginal posteriors plotted in Figure 2. In contrast to the previous result, the posteriors for L_p/L are centred around larger values of the parameter for

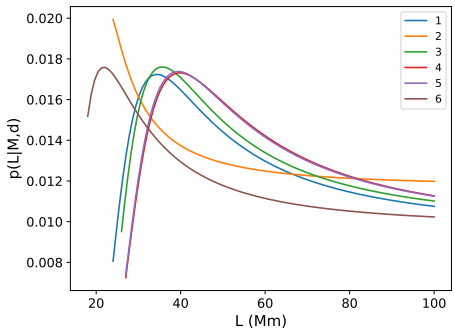

Figure 3: Posterior distributions of L for oscillating and flowing threads observed by [5]. An observation time of 180 s and a ratio $P(t)/P(0) = 0.9$ with an uncertainty of 10% have been considered.

larger values of the period ratio. The same trend is observed for ρ_p/ρ_c, with a very small probability for values larger than 200.

2.3 Lengths in a partially filled tube with flow

Observations show that threads are not steady, they flow through prominence. This plasma flow introduces the necessity of considering the temporal dependence of wave periods. Theory [10] predicts an analytical expression for the change in period of the form

$$\frac{P(t)}{P(0)} = \sqrt{1 - \frac{4v_0^2 t^2}{(L + \frac{1}{3}L_p)(L - L_p)}}. \tag{7}$$

The observable, $d = P(t)/P(0)$, is a function of three parameters, the flow velocity, v_0, the length of the thread, L_p, and the total length of the flux tube, L, $\theta = \{v_0, L_p, L\}$. In this particular case, Gaussian priors for v_0 and L_p are assumed using measurements by [5] for the computation of marginal posteriors of L in Figure 3. Posteriors are not properly inferred since they show long and high tails. However, they show a common tendency to peak at around 20 to 40 Mm, with the shortest threads supporting the smallest flow velocities.

3 Model Comparison

3.1 Period ratios in the short and long thread limits

In section 2.2, we made parameter inference using period ratios under the long and short thread approximations. To compare the two approximations, we compute marginal likelihoods and Bayes' factors in Figure 5. Period ratios smaller than 0.5 and larger than 2 are more likely for the short thread limit, while period ratios around 1 are better explained by the long thread limit.

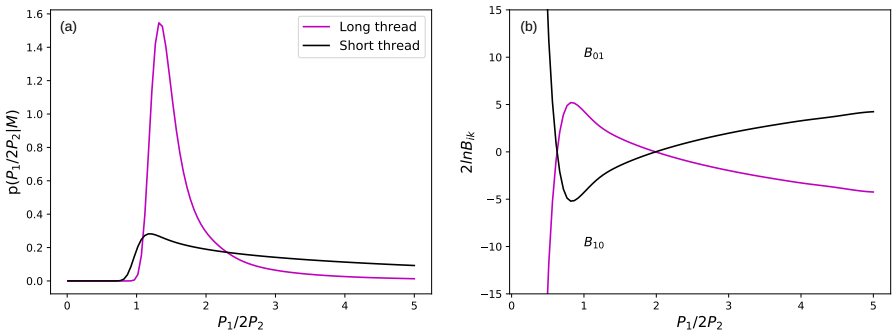

Figure 4: Marginal likelihoods (a) and Bayes' factors (b) for long and short thread approximations. $P_1/2P_2 \in [0.01, 5]$ with an uncertainty of 10%.

3.2 Damping mechanisms

Damping of transverse waves is a common observed phenomenon in prominence threads but the causative mechanism is not well known. We consider as plausible mechanisms resonant absorption in the Alfvén continuum, resonant absorption in the slow continuum, and Cowling's diffusion to derive which one is more plausible in explaining observed damping ratios, $d = \tau_d/P$. Theoretical damping ratios [1, 7, 8, 9] for these three cases are

$$\left(\frac{\tau_d}{P}\right)_{RAAC} = \frac{2}{\pi}\frac{R}{l}; \quad \left(\frac{\tau_d}{P}\right)_{RASC} = \frac{2}{\pi}\frac{R}{l}\left(\frac{k_z R}{1+\frac{2}{\gamma\beta}}\right)^{-2}; \quad \left(\frac{\tau_d}{P}\right)_{CD} = \frac{\sqrt{2}}{\pi k_z R \tilde{\eta}_c}, \tag{8}$$

respectively. Computed marginal likelihoods for each damping mechanism are presented in Figure 5a-c. Each marginal likelihood peaks around well differentiated damping ratio values, so that resonant absorption in the slow continuum can be directly discarded.

The remaining mechanisms are compared using Bayes' factors in Figure 5d. Damping ratios smaller than 10 are more plausible for resonant absorption in the Alfvén continuum and the rest for the Cowling's diffusion.

4 Conclusions

Applying Bayesian techniques to the study of prominence threads, magnetic field strengths of units to few tens of Gauss are obtained in quiescent prominences. When we use period ratios to infer the length of the threads, different tendencies in long and short approximations are observed. Introducing flows, the inferred total length of flux tubes in an active prominence region indicate they are shorter than expected.

Model comparison shows differences of periods ratio values in short and long thread limits and resonant absorption in the Alfvén continuum as the most plausible mechanism for explaining damping of transverse waves.

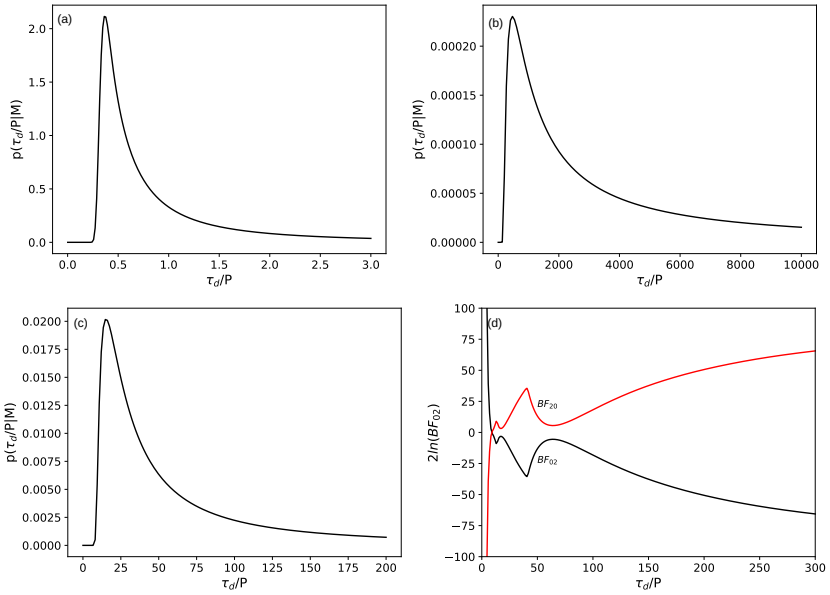

Figure 5: (a)-(c) Marginal likelihoods associated to each damping mechanism. Ranges of damping ratios are displayed in x-axis. (d) Bayes' factors associated to resonant absorption in the Alfvén continuum and Cowling's diffusion comparison for $\tau_d/P \in [0.01, 300]$ with an uncertainty of 10%.

Acknowledgments

We acknowledge financial support from the Spanish Ministry of Economy and Competitiveness (MINECO) through projects AYA2014-55456-P (Bayesian Analysis of the Solar Corona), AYA2014-60476-P (Solar Magnetometry in the Era of Large Telescopes), and from FEDER funds. M.M-S. acknowledges financial support through a Severo Ochoa FPI Fellowship under the project SEV-2011-0187-03.

References

[1] Arregui, I., Terradas, J., Oliver, R., et al. 2008, ApJ, 682, L141

[2] Arregui, I., Oliver, R., & Ballester, J. L. 2018, Living Reviews in Solar Physics, 15, 3.

[3] Díaz, A. J., Oliver, R. & Ballester, J. L. 2010, ApJ, 725, 1742

[4] Lin, Y., Soler, R., Engvold, O., et al. 2009, ApJ, 704, 870

[5] Okamoto, T. J., Tsuneta, S., Berger, T. E., et al. 2007, Science, 318, 1577

[6] Okamoto, T. J., Antolin, P., De Pontieu, B., et al. 2015, ApJ, 809, 71

[7] Soler, R., Oliver, R., Ballester, J. L., et al. 2009, ApJ, 695, L166

[8] Soler, R., Oliver, R. & Ballester, J. L. 2009, ApJ, 693, 1601

[9] Soler, R., Oliver, R. & Ballester, J. L. 2009, ApJ, 707, 662

[10] Soler, R. & Goossens, M. 2011, aap, 531, A167